Virginia Commonwealth University
VCU Scholars Compass

2012

Determination of the absolute internal quantum efficiency of photoluminescence in GaN co-doped with Si and Zn

M. A. Reshchikov
Virginia Commonwealth University, mreshchikov@vcu.edu

M. Foussekis
Virginia Commonwealth University

J. D. McNamara
Virginia Commonwealth University, mcnamarajd@vcu.edu

See next page for additional authors

Follow this and additional works at: http://scholarscompass.vcu.edu/phys_pubs

Part of the Physics Commons

Downloaded from

http://scholarscompass.vcu.edu/phys_pubs/124

Authors

M. A. Reshchikov, M. Foussekis, J. D. McNamara, A. Behrends, A. Bakin, and A. Waag

Determination of the absolute internal quantum efficiency of photoluminescence in GaN co-doped with Si and Zn

M. A. Reshchikov,[1,a)] M. Foussekis,[1] J. D. McNamara,[1] A. Behrends,[2] A. Bakin,[2] and A. Waag[2]

[1]*Physics Department, Virginia Commonwealth University, Richmond, Virginia 23284, USA*
[2]*Institute of Semiconductor Technology, Technische Universität Braunschweig, Braunschweig, Germany*

The optical properties of high-quality GaN co-doped with silicon and zinc are investigated by using temperature-dependent continuous-wave and time-resolved photoluminescence measurements. The blue luminescence band is related to the Zn_{Ga} acceptor in GaN:Si,Zn, which exhibits an exceptionally high absolute internal quantum efficiency (IQE). An IQE above 90% was calculated for several samples having different concentrations of Zn. Accurate and reliable values of the IQE were obtained by using several approaches based on rate equations. The concentrations of the Zn_{Ga} acceptors and free electrons were also estimated from the photoluminescence measurements. © *2012 American Institute of Physics*. [http://dx.doi.org/10.1063/1.3699312]

I. INTRODUCTION

Over the past three decades, GaN and other nitrides have attracted great interest as materials for short-wavelength light-emitting diodes and laser diodes. Significant efforts are currently being made to increase the internal quantum efficiency (IQE) in these light-emitting devices. However, from a number of methods commonly used to determine the IQE of electroluminescence or photoluminescence (PL) from GaN-based materials or light-emitting devices, only a few appear to be reliable and provide accurate estimates of the IQE.[1] Often, the ratio of the room-temperature and low-temperature PL intensities is used as a rough estimate of the *relative* IQE. There is no consensus in the literature on a reliable method of determining the *absolute* IQE of the PL in GaN. High values of the absolute IQE (30–70%) were reported for InGaN/GaN quantum wells.[2–5] However, assumptions made in these publications require more justification.[1]

In this work, we report on the extremely high absolute IQE of the PL in degenerate *n*-type GaN co-doped with Si and Zn. In our previous work,[6] preliminary results were reported on the IQE for one sample (sample 1008). In this work, two groups of GaN:Si,Zn samples (capped and uncapped), as well as GaN:Si samples were studied. The IQE was determined from the analysis of the dependencies of the PL intensity on the excitation intensity and temperature. The absolute IQE of the PL in GaN:Si,Zn exceeds 90%, with the largest contribution coming from the blue luminescence (BL) band. In addition, we demonstrate the versatility of the PL technique as a characterization tool for semiconductors. In particular, the concentrations of free electrons, shallow donors, and Zn_{Ga} acceptors in GaN doped with only Si or co-doped with Si and Zn have been determined from PL measurements.

II. EXPERIMENT

The eight GaN:Si,Zn samples analyzed in this work (Table I) were grown by metalorganic vapor phase epitaxy (MOVPE) on *c*-plane sapphire substrates at the Technische Universität Braunschweig (TUBS). Ammonia (NH_3), trimethylgallium (TMGa), SiH_4, and DeZn were used as the sources of N, Ga, Si, and Zn, respectively. For the four samples of group A, a 2 μm-thick undoped GaN layer was grown, and subsequently a 0.4 μm-thick AlGaN insulating barrier was deposited. The growth was finished with a 0.2 μm-thick GaN:Si,Zn active layer. The four samples of group B had the same structure, but were additionally capped with a 40 nm-thick AlGaN barrier. The DeZn flow rate during the growth of the GaN:Si,Zn layer was varied from 4 to 66 μmol/min for samples in each group to vary the concentration of Zn acceptors (Table I). Additionally, we studied a control sample which was grown under the same conditions, but with only Si doping of the active layer (sample 1150); as well as another Si-doped GaN sample grown by hydride vapor phase epitaxy (HVPE) at TDI, Inc. (sample 2015). The concentrations of free electrons in the GaN:Si,Zn layer for the samples in group A and in the Si-doped GaN samples have been found from the Hall effect measurements (Table I). All of the samples were degenerate, except for sample 2015. The concentration of electrons in the GaN:Si,Zn samples from group B could not be determined by the Hall effect measurements because of the insulating AlGaN capping layer. However, the electron concentration in these samples was estimated from time-resolved PL measurements to be about 10^{19} cm^{-3}, as will be demonstrated in Sec. III C.

Steady-state PL was excited with a 50 mW He-Cd laser, dispersed by a 1200 rules/mm grating in a 0.3 m monochromator, and was detected by a cooled photomultiplier tube. By using calibrated neutral density filters and an unfocused laser beam with a diameter of 4 mm, the excitation power density (P_{exc}) was varied from 10^{-5} to 0.3 W/cm^2. The beam could be focused to a diameter of 0.1–0.2 mm to obtain an P_{exc} up to 200 W/cm^2. Time-resolved PL was excited with a pulsed nitrogen laser (337 nm) and analyzed with an oscilloscope. A closed-cycle optical cryostat and a high-temperature cryostat were employed to achieve sample temperatures of 15–330 K and 295–700 K, respectively. The PL

a)Electronic mail: mreshchi@vcu.edu.

TABLE I. Characteristics of GaN samples and PL.

Sample	DeZn flow (μmol /min)	Group	n from Hall (cm^{-3})	n from TR-PL (cm^{-3})	$N_1 \equiv N_{Zn}$ by method 1 (cm^{-3})	$N_1 \equiv N_{Zn}$ by method 2 (cm^{-3})	τ_1 at 200 K (μs)	T_0 (K)	E_{A1} (meV)
1143	4	A	1.03×10^{19}	1.3×10^{19}	7×10^{17}	2.9×10^{17}	0.52	289	310
1142	10	A	1.03×10^{19}	1.2×10^{19}	5×10^{17}	6.7×10^{17}	0.55	296	310
1141	33	A	1.14×10^{19}	9.5×10^{18}	1.5×10^{18}	1.3×10^{18}	0.70	313	340
1140	66	A	0.75×10^{19}	4.5×10^{18}	3×10^{18}	4.7×10^{18}	1.48	305	290
1010	4	B	–	1.8×10^{19}	1×10^{18}	5.0×10^{17}	0.37	289	320
1009	10	B	–	1.8×10^{19}	2×10^{18}	1.1×10^{18}	0.38	294	315
1008	33	B	–	1.4×10^{19}	5×10^{18}	2.0×10^{18}	0.47	300	300
997	66	B	–	5.2×10^{18}	1×10^{19}	5.3×10^{18}	1.27	311	345
1150	–	–	1.1×10^{19}	–	–	2×10^{13}	–	250	345
2015[a]	–	–	2×10^{17}	6×10^{17}	3×10^{15}	–	15	220	345

[a]5 μm-thick GaN:Si sample grown by HVPE method at TDI.

spectra were corrected for the response of the optical system by comparing the spectrum of a tungsten lamp with a standard spectrum.

III. RESULTS

A. Hall effect

In GaN:Si,Zn (group A) and GaN:Si samples grown at TUBS, the concentration of free electrons was in the range of $(0.75 - 1.14) \times 10^{19}$ cm^{-3} at room temperature (Table I); i.e., these samples are degenerate. As expected for degenerate semiconductors, the temperature dependence of the electron concentration is negligible (Fig. 1). The Hall mobility in these samples was about 150 cm^2/Vs at room temperature and slightly increased with decreasing temperature (Fig. 2).

Sample 2015 grown by the HVPE method at TDI contained a thin degenerate layer near the GaN/sapphire interface. This layer shunted the conductivity of the 5 μm-thick layer, indicated by a rise in the calculated concentration of free electrons with decreasing temperature.[7] Figures 1 and 2

show the corrected concentration of free electrons and the electron Hall mobility for the bulk region, excluding the degenerate layer. The description of the two-layer model can be found in Ref. 7, and a more detailed analysis of the Hall effect data for sample 2015 can be found in Ref. 8.

B. Steady-state photoluminescence

PL spectra from GaN:Si,Zn samples of group A at 200 and 320 K are shown in Fig. 3. The PL spectra from these samples were very similar to the spectra obtained from samples of group B. The PL spectra include a strong BL band with a maximum at 2.9 eV; a weak peak at higher photon energies, hereafter called the near-band edge (NBE) emission; and a broad yellow luminescence (YL) band with a maximum at about 2.1–2.2 eV. The YL band is attributed to a deep acceptor, which is most likely due to a complex defect involving a Ga vacancy.[9] The BL band is attributed to transitions from the conduction band (or shallow donors at very low temperatures) to the Zn$_{Ga}$ acceptor.[9,10] The shape of this band at different temperatures is well known,[9,10] and this information was used to deconvolute the bands before finding their integrated intensities in this work.
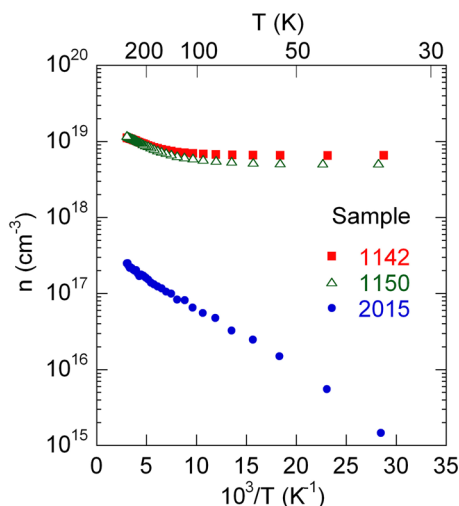

FIG. 1. Temperature dependence of the free-electron concentration in GaN:Si,Zn (sample 1142) and GaN:Si (1150) grown by MOVPE at TUBS and GaN:Si (2015) grown by HVPE at TDI. The data for sample 2015 are calculated by using a two-layer model.[7,8]
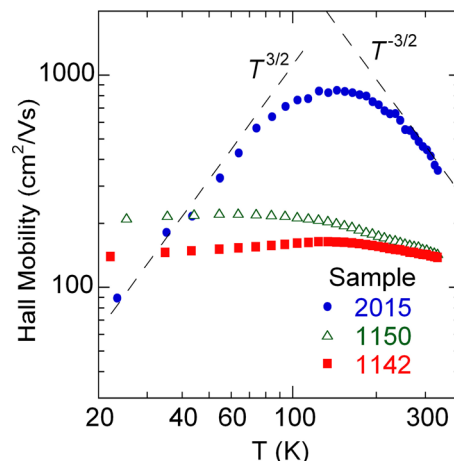

FIG. 2. Temperature dependence of the Hall mobility of electrons in three representative samples. The data for sample 2015 are calculated by using a two-layer model.[7,8]
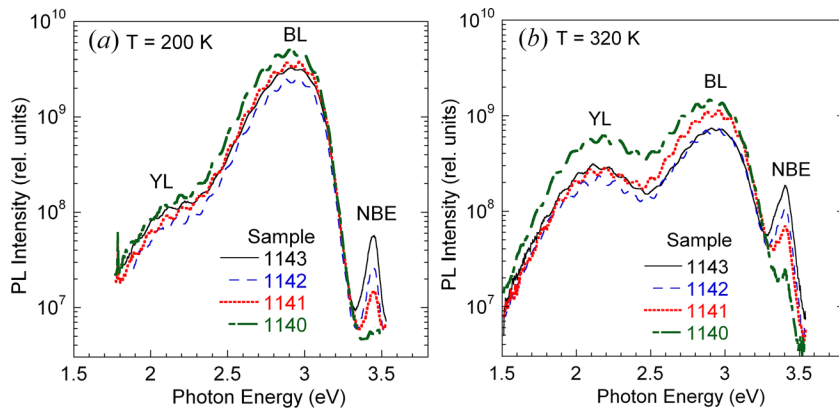
FIG. 3. PL spectra from four GaN:Si,Zn samples of group A at 200 K (a) and 320 K (b). $P_{exc} = 0.0015\,\text{W/cm}^2$.

The excitonic PL spectrum at low temperature is shown in Fig. 4 for sample 1142 at different excitation intensities. Two peaks could be identified in the spectrum. A peak at 3.456 eV is labeled as the acceptor bound exciton (ABE) and is attributed to an exciton bound to the Zn_{Ga} acceptor. The source of the peak at 3.484 eV is inconclusive: it might be due to the donor bound exciton (DBE), a free exciton (FE), or a combination of both. The peak at 3.456 eV is seen only at high excitation intensities when the Zn_{Ga} acceptors become saturated with holes, while the peak at 3.484 eV dominates at low excitation intensities.

PL spectra at 200 K for GaN samples doped only with Si are shown in Fig. 5. In the case of the MOVPE-grown GaN:Si sample, the NBE band was much stronger than that in the GaN:Si,Zn samples. Very small contributions of the BL band can be found near 2.9 eV in sample 1150 (shown with a dashed line in Fig. 5). The signal at 2.9 eV was independent of temperature between 160 and 220 K and was quenched at higher temperatures with an activation energy approximately equal to that of the BL band in other samples.

The PL spectrum of the HVPE-grown sample (2015) contains a weak and relatively narrow NBE band and a strong BL band. We have established that undoped and Si-doped GaN samples from TDI typically contain residual Zn (with concentrations on the order of 10^{15} cm^{-3}) which is responsible for the strong BL band.[9–11] At lower photon energies, we can see the red luminescence (RL) band of unknown origin which is also commonly present in undoped and Si-doped GaN samples grown at TDI.

Figure 6 shows the temperature dependence of the integrated PL intensity for the BL band in four GaN:Si,Zn samples, normalized at lower temperatures. The BL band intensity remains nearly constant when the temperature is increased from 15 to 250 K. This band is quenched at $T > 250$ K with an activation energy of about 300–340 meV. The characteristic temperature of the quenching, T_0, can be defined as the point where the low-temperature and high-temperature parts of the dependence cross when extrapolated as straight lines in the Arrhenius plot (Fig. 6). This value is unusually high ($T_0 = 300 \pm 10$ K) in the GaN:Si,Zn samples studied in this work (Table I), as compared to the earlier reported values ($T_0 = 200 - 220$ K).[9,12] As a comparison, we included in Fig. 6 the data for the Si-doped GaN (sample #2015) grown at TDI. Clearly, the T_0 in the GaN:Si,Zn samples is much higher than in samples with low concentrations of Zn and free electrons.
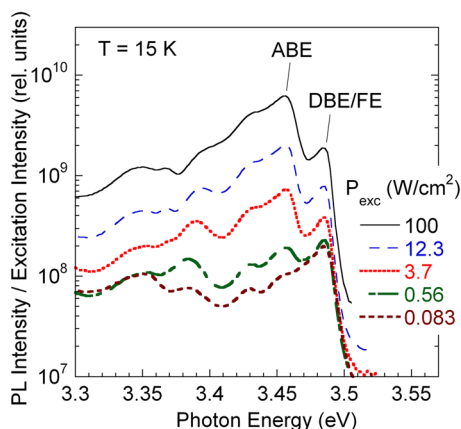

FIG. 4. Excitonic PL spectrum at $T = 15$ K and different excitation intensities for sample 1142. The PL intensity is normalized by dividing each spectrum by the corresponding excitation intensity. ABE is the acceptor (Zn_{Ga}) bound exciton, DBE is the donor (Si_{Ga}) bound exciton, FE is free exciton.
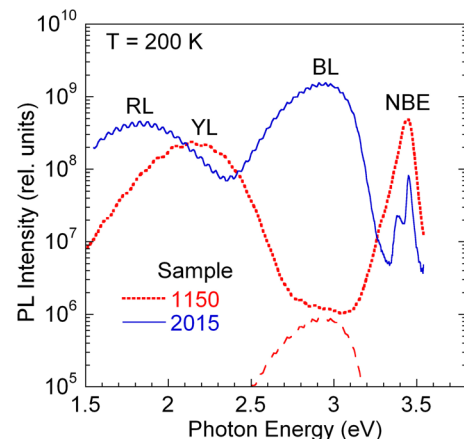

FIG. 5. PL spectra at 200 K for Si-doped GaN grown by MOVPE at TUBS (sample 1150) and HVPE at TDI (sample 2015). $P_{exc} = 0.0015\,\text{W/cm}^2$. Dashed curve shows the estimated contribution of the BL band to the spectrum of sample 1150 as found from a comparison of the PL spectra at different temperatures.
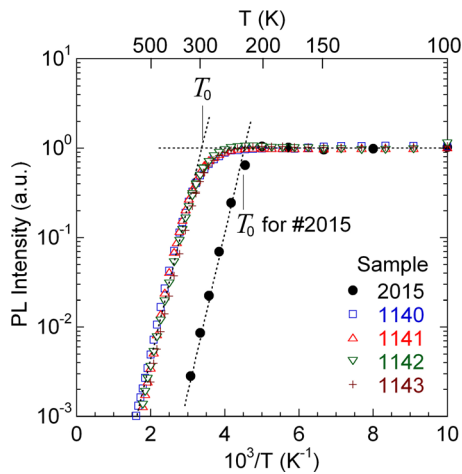
FIG. 6. Temperature dependence of the integrated PL intensity (normalized at temperatures below 100 K) for the BL band in four GaN:Si,Zn samples of group A and GaN:Si sample (#2015). $P_{exc} = 0.0015$ W/cm². $T_0 = 220$ K for sample 2015, and $T_0 \approx 300$ K for all other samples.

From 15 to 200 K, the NBE and YL band intensities slowly decrease with increasing temperature. However, at $T = 250 - 350$ K, simultaneously with the quenching of the BL band, both the NBE and YL bands exhibit a sharp rise by an order of magnitude and then decrease again at higher temperatures (Fig. 7). This stepwise behavior clearly indicates a very high IQE of the BL band.[12] In contrast, the intensity of the NBE and YL bands in the Si-doped GaN sample (1150) monotonously decreased with increasing temperature from 100 to 700 K, and no stepwise behavior was observed. The YL band in this sample was quenched at temperatures above 500 K with an activation energy of 500–550 meV, which is very similar to the simulated curve $\eta_{20}(T)$ shown in Fig. 7. Detailed analysis of the YL band behavior in undoped and
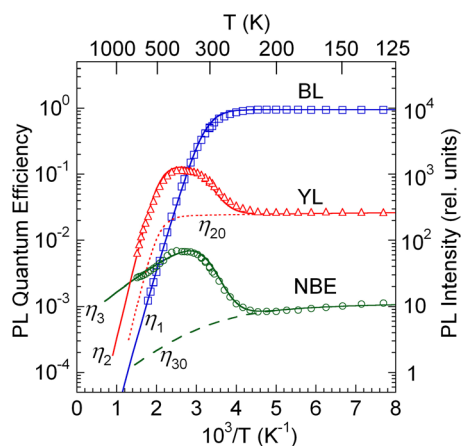

FIG. 7. Temperature dependence of the absolute IQE of PL in GaN:Si,Zn (sample 1141) at $P_{exc} = 0.0015$ W/cm². Points are experimental data. Solid blue curve shows η_1 calculated by using Eq. (7) with the following parameters: $\eta_{10} = 0.91$, $g = 2$, $C_{pA} = 7 \times 10^{-7}$ cm³/s, $\tau_1 = 0.7$ μs, $E_{A1} = 340$ meV. Dotted red and dashed green lines show $\eta_{20}(T)$ and $\eta_{30}(T)$ calculated by using Eq. (14) with the following parameters: $\eta_{20}(0) = 0.027$, $C_1 = 0.3$, $C_2 = 1.7 \times 10^5$, $E_1 = 15$, $E_2 = 500$ meV (for the YL band); $\eta_{30}(0) = 1.2 \times 10^{-3}$, $C_1 = 1$, $C_2 = 40$, $E_1 = 25$, $E_2 = 100$ meV (for the NBE band). $G = 2.4 \times 10^{20}$ cm⁻³ s⁻¹ and $\beta = 4.5 \times 10^{-17}$ for all the bands. Solid red and green lines show $\eta_2(T)$ and $\eta_3(T)$ calculated by using Eq. (17) with $\eta_{10} = 0.83$ and $\eta_{10} = 0.95$, respectively.

Si-doped GaN samples is beyond the scope of this work and will be reported elsewhere.

C. Time-resolved photoluminescence

In the studied samples, after pulsed excitation, the BL band intensity decays nearly exponentially. To more accurately find the characteristic lifetime of the BL band, we plotted the product of PL intensity and time as a function of time delay. The PL lifetime was determined from the position of the maximum in this plot.[13] The PL lifetime is almost constant at $T < T_0$ (Fig. 8). However, at temperatures above T_0, the lifetime decreases with a slope corresponding to the activation energy of the Zn_{Ga} acceptor. The temperature dependencies of the PL lifetime and PL intensity were very similar to each other.

The PL lifetime in *n*-type semiconductors is inversely proportional to the concentration of free electrons.[13] The weak decrease of the PL lifetime with increasing temperature from 100 to 200 K in sample 2015 can be explained by the corresponding increase in the concentration of free electrons. In the degenerate sample 1142, the PL lifetime was nearly independent of temperature, in the range of 100–250 K, which agrees with the constant concentration of free electrons in this sample.

D. Dependence of the photoluminescence intensity on excitation intensity

We have also studied the effect of excitation intensity on the PL intensity for each PL band at different temperatures. The YL band intensity increases linearly at low excitation intensities but begins saturating at $P_{exc} > 10^{-4} - 10^{-3}$ W/cm². This saturation can be explained by a number of reasons, including the following: a low concentration of the related defects, the long PL lifetime (greater than 10 μs) and the possible contribution from donor-acceptor pair transitions to this band. In contrast, the BL and NBE band intensities increase linearly with the excitation intensity up to $0.1 - 1$ W/cm². Figure 9 shows the ratio of the integrated PL intensity and the excitation intensity as a function of the excitation power density for the NBE and BL bands in four GaN:Si,Zn samples of group A at 200 K. This ratio is proportional to the
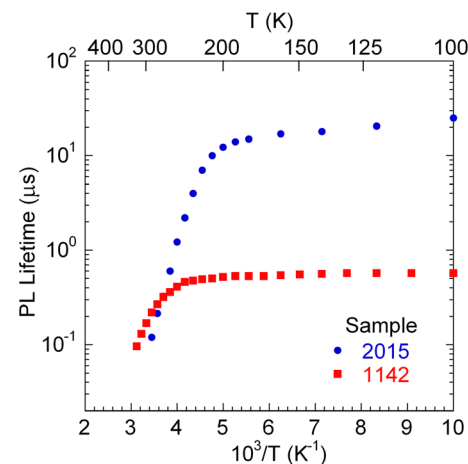

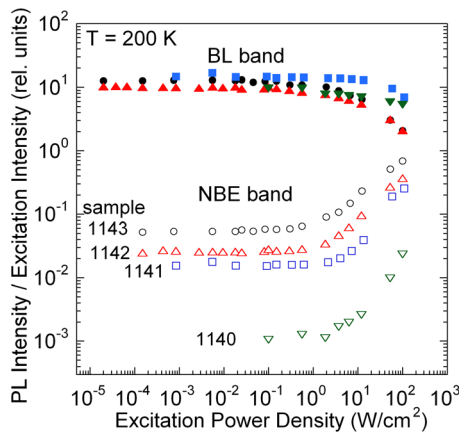FIG. 8. Temperature dependence of PL lifetime for the BL band in GaN.

FIG. 9. Integrated PL intensity divided by the excitation intensity as a function of excitation power density for NBE and BL bands in four GaN:Si,Zn samples at $T = 200$ K. Solid symbols represent the BL band and empty symbols represent the NBE band.

IQE of PL. We can see that the IQE of the BL band starts decreasing above $P_{exc} \approx 1$ W/cm^2. Simultaneously, the IQE of the NBE band increases. As will be shown in Sec. IV C, this behavior is the result of a competition between recombination channels, and it also indicates a very high IQE of the BL band.

IV. MODEL

A. Rate equations

Let us consider *n*-type GaN which contains shallow Si$_{Ga}$ donors with concentration N_D, Zn$_{Ga}$ acceptors responsible for the BL band with concentration N_{A1}, deep acceptors responsible for the YL band with concentration N_{A2}, and one (dominant) type of nonradiative centers, S, with concentration N_S. The variables N_D^+, N_D^0, N_{A1}^-, N_{A1}^0, N_{A2}^-, N_{A2}^0, N_S^-, and N_S^0 are the concentrations of these centers in different charge states. For definiteness, we assumed that the nonradiative centers are acceptors in an *n*-type semiconductor.

Under continuous illumination, electron-hole pairs are produced with a generation rate G per unit volume. The steady-state concentrations of free electrons and holes are n and p, respectively. We traditionally describe the transition rates as the product of the concentrations of available carriers and available empty sites, multiplied by a constant factor called the capture coefficient.[14,15] In particular, holes are captured by the Zn$_{Ga}$ acceptors, YL-related acceptors, and nonradiative centers at rates $C_{pA1}N_{A1}^-p$, $C_{pA2}N_{A2}^-p$, and $C_{pS}N_S^-p$, where C_{pA1}, C_{pA2}, and C_{pS} are the hole-capture coefficients for the Zn$_{Ga}$ acceptor, the YL-related acceptor, and the nonradiative center S, respectively. In addition, free holes and electrons may recombine directly or form excitons. The rate of these processes will be described as Bnp, where the rate coefficient B includes both the exciton and free electron-hole recombination components.[16] Holes captured by acceptors, nonradiative defects, or excitons, may return to the valence band as a result of thermal excitation. We will explicitly consider only the thermal emission of holes from the Zn$_{Ga}$ acceptors to the valence band at the rate Q_{A1},[10] where Q_{A1} is defined as

$$Q_{A1} = C_{pA1}N_v g^{-1} \exp\left(-\frac{E_{A1}}{kT}\right), \qquad (1)$$

where E_{A1} is the ionization energy of the Zn$_{Ga}$ acceptor, N_v is the effective density of states in the valence band, g is the degeneracy factor of the acceptor level (assumed to be equal to 2), T is the temperature, and k is Boltzmann's constant.

The rate equations under steady-state conditions can be constructed with the same approach as in Refs. 10 and 12. The rate of change of the free-hole concentration in the valence band in the steady-state condition is given by

$$\frac{dp}{dt} = G - C_{pA1}N_{A1}^-p - C_{pA2}N_{A2}^-p - C_{pS}N_S^-p$$
$$- Bnp + Q_{A1}N_{A1}^0 = 0. \qquad (2)$$

The rate of change of the free electron concentration in the conduction band is given by

$$\frac{dn}{dt} = G - C_{nA1}N_{A1}^0 n - C_{nA2}N_{A2}^0 n - C_{nS}N_S^0 n - Bnp = 0, \quad (3)$$

where C_{nA1}, C_{nA2}, and C_{nS} are the electron capture coefficients for the Zn$_{Ga}$ acceptor, the YL-related acceptor, and nonradiative center S, respectively. Capture of electrons by shallow donors D, and the thermal emission of electrons from shallow donors to the conduction band are not relevant in the case of a degenerate *n*-type semiconductor. It is also assumed that the concentration of photogenerated electrons in the conduction band, δn, is much smaller than the concentration of free electrons in the dark, n_0, so that $n \approx n_0$. We can also introduce the characteristic lifetime of luminescence which is related to electron transitions from the conduction band to the Zn$_{Ga}$ acceptors as $\tau_{A1} = (C_{nA1}n)^{-1}$.[13] Similarly, the characteristic lifetimes of the YL and NBE emission and nonradiative recombination, can be defined as $\tau_{A2} = (C_{nA2}n)^{-1}$, $\tau_{NBE} = (Bn)^{-1}$ and $\tau_S = (C_{nS}n)^{-1}$, respectively.

To simplify the notation in Eqs. (2) and (3), we will number the recombination channels via the Zn$_{Ga}$ acceptor, YL-related acceptor, exciton (or free electron-hole recombination), and nonradiative center S as 1, 2, 3, and 4, respectively. Then, we will let C_{pi} ($i = 1, 2, 3, 4$) represent $C_{p1} \equiv C_{pA1}$, $C_{p2} \equiv C_{pA2}$, $C_{p3} \equiv B$, $C_{p4} \equiv C_{pS}$; τ_i represent $\tau_1 \equiv \tau_{A1}$, $\tau_2 \equiv \tau_{A2}$, $\tau_3 \equiv \tau_{NBE}$, $\tau_4 \equiv \tau_S$; and $Q_1 \equiv Q_{pA1}$. Further, in Eq. (2) we let N_i^- represent N_{A1}^-, N_{A2}^-, n, and N_S^-, while in Eq. (3) we let N_i^0 represent N_{A1}^0, N_{A2}^0, p, and N_S^0, for the channels with $i = 1, 2, 3$, and 4, respectively. By using this compact notation for the four recombination channels, Eqs. (2) and (3) can be replaced with the following expressions:

$$\frac{dp}{dt} = G - \sum_{i=1}^{4} C_{pi}N_i^-p + Q_1 N_1^0 = 0, \qquad (4)$$

and

$$\frac{dn}{dt} = G - \sum_{i=1}^{4} \frac{N_i^0}{\tau_i} = 0. \qquad (5)$$

The four main recombination channels in GaN:Si,Zn have the absolute IQE η_i. The intensity of the BL band, I_1, is

$$I_1 = \frac{N_1^0}{\tau_1} = C_{p1}N_1^- p - Q_1 N_1^0 \qquad (6)$$

and its IQE is $\eta_1 = I_1/G$. The temperature dependence of the IQE of the BL band, $\eta_1(T)$, in n-type GaN can be described with the formula[10,12]

$$\eta_1(T) = \frac{\eta_{10}}{1 + (1 - \eta_{10})\tau_1 Q_1}, \qquad (7)$$

where η_{10} is the IQE of the BL band at low temperatures ($T < 200\,\mathrm{K}$) when $Q_1 \approx 0$. When this dependence is plotted as an Arrhenius plot (logarithm of PL intensity or IQE as a function of inverse temperature), two regions can be distinguished: a region where the IQE of the BL band is independent of temperature at $T < T_0$,

$$\eta_1(T < T_0) = \eta_{10} = C_{p1}N_1^- p/G, \qquad (8)$$

and a region where the BL band is quenched with an activation energy close to E_{A1}

$$\eta_1(T > T_0) \approx \frac{\eta_{10} g}{(1 - \eta_{10})\tau_1 C_{p1}N_v} \exp\left(\frac{E_{A1}}{kT}\right). \qquad (9)$$

Note that in Eq. (9) the temperature dependence of N_v is weak as compared to the exponential dependence. The characteristic temperature T_0 can be found from the condition

$$(1 - \eta_{10})\tau_1 Q_1 = 1 \qquad (10)$$

and defined as the temperature at which the low-temperature and high-temperature parts in the Arrhenius plot cross when extrapolated as straight lines (Fig. 6).
The IQE of the YL band is

$$\eta_2 = C_{p2}N_2^- p/G, \qquad (11)$$

and the IQE of the NBE emission is

$$\eta_3 = Bnp/G, \qquad (12)$$

where the coefficient B is a function of temperature.
Finally, the absolute efficiency of the nonradiative recombination is

$$\eta_4 = C_{p4}N_4^- p/G. \qquad (13)$$

The PL intensity integrated over a spectral region of a particular PL band, I_i^{PL}, is proportional to its absolute IQE, and can be expressed as $I_i^{PL} = \beta\eta_i G$, where β is a constant determined by the total collection efficiency of luminescence (assumed to be independent of temperature and the same for all channels).

B. Dependence of the PL intensity on temperature

We define η_{i0} and I_{i0}^{PL} ($I_{i0}^{PL} = \beta\eta_{i0}G$) as the temperature-dependent absolute IQE and corresponding integrated PL intensity for the ith channel ($i = 1, 2, 3$) in the case where the BL band *is not* quenched and the subsequent redistribution of the minority carriers (holes) between different channels *does not* occur. However, the quenching of the BL band does cause a redistribution of the holes, which consequently changes the efficiencies of all recombination channels. The temperature-dependent values η_i and I_i^{PL} will include the effect of the BL band quenching.

In practice, the temperature dependence of I_{i0}^{PL} for $i \neq 1$ can be found by modeling the experimentally found $I_i^{PL}(T)$ dependence at temperatures below the quenching of the BL band with the following expression:

$$I_{i0}^{PL}(T) = \frac{I_{i0}^{PL}(0)}{1 + A_1 e^{-E_1/kT} + A_2 e^{-E_2/kT}} \qquad (14)$$

and by extrapolating this dependence to higher temperatures. Here, $I_{i0}^{PL}(0) = \beta\eta_{i0}(0)G$ is the integrated PL intensity in the low-temperature limit and A_1, A_2, E_1, and E_2 are fitting parameters that determine the positions and slopes of the lines in the Arrhenius plot. The $I_{i0}^{PL}(T)$ [or $\eta_{i0}(T)$] dependencies for the YL ($i = 2$) and NBE ($i = 3$) bands are shown in Fig. 7 with dotted and dashed curves, respectively. By using this formal approach, we leave out the explanation of the changes in PL intensities with temperature for the PL bands with $i \neq 1$, which are not directly related to the quenching of the BL band but may be related to dissociation of excitons (for the NBE emission), slow variation in coefficients C_{pi}, or any other reasons. Moreover, since the thermal emission of holes to the valence band was not explicitly included in Eq. (4) for channels with $i \neq 1$, we can postulate that the temperature dependence described with Eq. (14) is included in parameters B and C_{pi} in Eqs. (11)–(13).

Since $\sum_{i=1}^4 \eta_i = 1$, and each term η_i with $i > 1$ contains the hole concentration p as a factor, we can express p from Eqs. (4) and (6) as

$$p = \frac{G(1 - \eta_1)}{C_{p2}N_2 + Bn + C_{p4}N_4}, \qquad (15)$$

where we replaced N_i^- with N_i, which is justified for low excitation intensities when defects are not saturated with holes and the relative concentration of holes bound to the YL-related acceptor and nonradiative center S is negligible. Then, we can substitute p from Eq. (15) into the expressions for the IQE of any channel with $i \neq 1$ [Eqs. (11)–(13) with $N_i^- = N_i$]. In the region of substantial thermal quenching of the BL band ($T \approx 250 - 350\,\mathrm{K}$), the intensities of other PL bands increase, because η_1 in Eq. (15) decreases. If the BL band was not quenched, concentration of holes p_0 would be described by Eq. (15) with $\eta_1 = \eta_{10}$; i.e.,

$$p_0 = \frac{G(1 - \eta_{10})}{C_{p2}N_2 + Bn + C_{p4}N_4}, \qquad (16)$$

and the efficiencies of channels with $i = 2, 3$, and 4 would be, $\eta_{20} = C_{p2}N_2 p_0/G$, $\eta_{30} = Bn p_0/G$, and $\eta_{40} = C_{p4}N_4 p_0/G$, respectively. Thus, by dividing η_i by η_{i0} and canceling out the terms that have the same temperature dependence, we can express the *relative change* of the integrated PL intensity I_i^{PL}/I_{i0}^{PL} ($i = 2, 3$) due to the quenching of the BL band as

$$\frac{I_i^{PL}}{I_{i0}^{PL}} = \frac{\eta_i}{\eta_{i0}} = \frac{1 - \eta_1}{1 - \eta_{10}}. \quad (17)$$

Note that, according to Eq. (17), the I_i^{PL}/I_{i0}^{PL} ratios and their temperature dependencies are identical for all of the recombination channels with $i > 1$. Recalling that $\eta_1 = (I_1^{PL}/I_{10}^{PL})\eta_{10}$, we see that η_{10} is the only fitting parameter in the fit of the experimentally found $I_i^{PL}(T)$ dependencies with Eq. (17) for channels with $i > 1$, provided that we have the temperature dependencies of I_1^{PL}/I_{10}^{PL} and $I_{i0}^{PL}(T)$ in relative units.

C. Dependence of PL intensity on excitation intensity

Remarkably, Eq. (17) can be used not only in the case of the thermal quenching of the BL band but also in the case of its "quenching" by high excitation intensity. Indeed, the IQE of the defect-related PL band decreases with increasing excitation intensity above some critical value G_0, due to saturation of the defect with photogenerated holes.[9] The dependence of η_1 on G can be described with a simple model which assumes that within an active layer of thickness α^{-1} the generation rate G is constant, where α is the absorption coefficient. In application to the BL band in GaN:Si,Zn, it can be shown that the $\eta_1(G)$ dependence is[9]

$$\eta_1 = \frac{1}{2}\left(1 + \frac{N_1}{G\tau_1\eta_{10}}\right) - \sqrt{\frac{1}{4}\left(1 + \frac{N_1}{G\tau_1\eta_{10}}\right)^2 - \frac{N_1}{G\tau_1}}, \quad (18)$$

where η_{10} is the IQE of the BL band in the limit of low excitation intensities when the BL band intensity increases linearly with the excitation intensity. Remarkably, when η_{10}, G, and τ_1 are known, the concentration of the Zn_{Ga} acceptors (N_1) can be estimated from the fit of the $\eta_1(G)$ dependence with Eq. (18).

However, the above approximation introduces some error because the complete saturation of the PL intensity at $G \gg G_0 = N_1/(\tau_1\eta_{10})$ predicted by Eq. (18) is never observed in the experiment. This is because the excitation intensity decreases exponentially inside the semiconductor.[17] This phenomenon can be accounted for by replacing G with $G(x)$, where x is the distance from the semiconductor surface into the bulk, and by integrating Eq. (18) over the entire thickness of a semiconductor layer.[17] In this method, we plot the IQE of the PL as a function of the excitation intensity $P_0 = P_{exc}/h\nu_{exc}$, where $h\nu_{exc}$ is the photon energy of the excitation light, and is expressed by the number of photons per unit time, per unit area. An example of the fit of the $\eta_1(P_0)$ dependence with the numerical integration of Eq. (18) [in which $G(x) = \alpha P_0 e^{-\alpha x}$] is shown in Fig. 10.

The saturation of the BL band intensity (or decrease of its IQE) with increasing excitation intensity can be interpreted as the quenching of the BL-related recombination channel. This effect is very similar to the *thermal* quenching of the BL band. Thus, it should result in an equal rise in the recombination rate for all other channels. The latter is described with Eq. (17) which is the same for the quenching of the BL band by temperature and excitation intensity, because it does not distinguish between different sources that reduce η_1. From the fit of the experimental $\eta_i(P_0)$ dependence with Eq. (17) we can find the IQE of the BL band in the limit of the low excitation intensity (η_{10}). This method is especially good when η_{i0} ($i \neq 1$) is independent of the excitation intensity for a wide range, which is expected for the NBE emission in a degenerate *n*-type semiconductor.
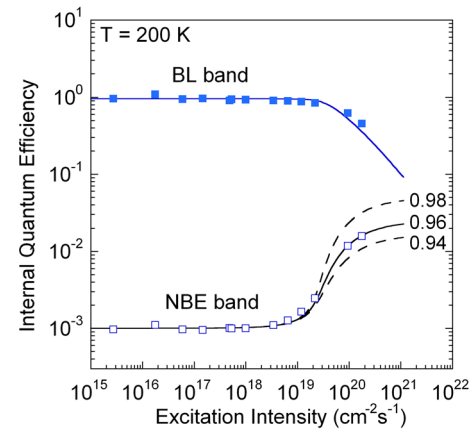

FIG. 10. Dependence of the IQE of PL on excitation intensity for the NBE and BL bands in GaN:Si,Zn (sample # 1141) at $T = 200$ K. Fit of the BL band is obtained by integrating Eq. (18) over the sample thickness with the following parameters: $\tau_1 = 0.7$ μs, $\eta_{10} = 0.96$, and $N_1 = 1.5 \times 10^{18}$ cm^{-3}. Solid curve for the NBE band shows $\eta_3(G)$ calculated by using Eq. (17) with $\eta_{30} = 10^{-3}$ and $\eta_{10} = 0.96$. Dashed curves show the fit with $\eta_{10} = 0.98$ and 0.94, as indicated in the figure.

V. DISCUSSION

A. Determination of the absolute IQE of photoluminescence

We can determine the absolute IQE of different PL bands, as well as the efficiency of nonradiative recombination, from four independent methods: (1) from the position of the characteristic temperature, T_0, in the $I_1^{PL}(T^{-1})$ dependence; (2) from the fit of the temperature dependence of the YL band intensity; (3) from the fit of the temperature dependence of the NBE band intensity; and (4) from the fit of the dependence of the NBE band intensity on excitation intensity. The results are summarized in Table II.

1. Characteristic temperature of the quenching of the BL band

In the GaN:Si,Zn samples used in this study, the quenching of the BL band begins at much higher temperatures ($T_0 = 300$ K) than it is commonly observed (200–220 K);[9,13] see Fig. 6. This can be partially explained by a short PL lifetime (due to a high concentration of free electrons). However, the main reason for the significant change in T_0 is the exceptionally high IQE of the BL band. In the fitting of the

TABLE II. Absolute IQE of PL at 200 K.

Sample	DeZn flux	From $I_1^{PL}(T)$	From $I_2^{PL}(T)$	From $I_3^{PL}(T)$	From $I_3^{PL}(P_0)$	Weighted average and error	From $\frac{I_{10}^{PL}}{I_{30}^{PL}}$
				η_{10}			η_{30}
1143	4	0.91	0.88	0.92	0.93	$0.92^{+0.01}_{-0.04}$	0.006
1142	10	0.94	0.83	0.92	0.95	$0.94^{+0.01}_{-0.03}$	0.0024
1141	33	0.91	0.83	0.95	0.96	$0.95^{+0.01}_{-0.03}$	0.001
1140	66	0.99	0.88	0.88	0.97	$0.96^{+0.01}_{-0.04}$	0.00013
1010	4	0.80	0.65	0.80	0.85	$0.81^{+0.02}_{-0.05}$	0.0042
1009	10	0.89	0.85	0.85	0.87	$0.86^{+0.02}_{-0.05}$	0.002
1008	33	0.96	0.93	0.92	0.9	$0.91^{+0.01}_{-0.04}$	0.0009
997	66	0.94	0.91	0.94	0.93	$0.93^{+0.01}_{-0.05}$	0.00013
2015	–	<0.2	<0.5	<0.5	–	$0.3^{+0.1}_{-0.2}$	

BL intensity with Eq. (7), the fitting parameters were E_{A1} (determines the slope of the high-temperature part of the Arrhenius plot) and η_{10} (determines the position of T_0). The value of C_{p1} for the BL band in undoped GaN has been estimated as $(9\pm3) \times 10^{-7}$ cm^3/s in Ref. 12 from analysis of the temperature dependencies of the BL band intensity in four samples grown by the MOVPE method. Since that time, we have analyzed the Zn-related BL band in many other GaN samples, including undoped, Si-doped and Zn-doped GaN grown by the MOVPE and HVPE methods. Based on these extensive data, we will slightly revise the value of C_{p1}, and instead use $C_{p1} = 7 \times 10^{-7}$ cm^3/s in this work. The values of η_{10} obtained with this method [η_{10} from $I_1^{PL}(T)$] are listed in the third column of Table II. When η_{10} is of the order of 0.1 or smaller, only the upper bound for η_{10} can be estimated ($\eta_{10} < 0.2$ for sample 2015) because the $I_1^{PL}(T)$ dependencies with $\eta_{10} = 0.2$ and $\eta_{10} = 0$ cannot be distinguished reliably while accounting for reasonable errors in the fixed and fitting parameters.

2. Enhancement of the YL band due to the quenching of the BL band

The intensity of the YL band in GaN:Si,Zn remained nearly unchanged with increasing temperature from 15 to 250 K. Remarkably, close to $T = T_0$, a stepwise rise in the YL band intensity is observed simultaneously with the quenching of the BL band (Fig. 7). At higher temperatures ($T > 500$ K), the YL band was quenched with the activation energy of 500–600 meV in almost all of the samples. The quenching could be explained by the thermal emission of holes from the YL-related acceptor to the valence band. It is beyond the scope of this work to discuss the details of this quenching and to identify the YL-related defect. What is important is the similar stepwise increase of the YL and NBE emission intensities by about an order of magnitude at temperatures close to $T = T_0$, which unambiguously indicates the very high absolute IQE of the BL band. From the fit of the experimental dependence of the YL band intensity with Eq. (17) (shown in Fig. 7 with a red solid curve labeled η_2), we find $\eta_{10} = 0.83$ for the absolute IQE of the BL band in sample 1141. The parameter η_{10} for other samples was estimated with the same procedure, and the values are listed in column 4 of Table II. There is no YL band

in the PL spectrum of sample 2015. However, the RL band showed a small increase (by up to a factor of two) in the region where the BL band was quenched, which allows us to estimate that $\eta_{10} < 0.5$ in this sample.

3. Enhancement of the NBE emission due to the quenching of the BL band

The integrated intensity of the NBE emission decreases with increasing temperature, which could be attributed to the dissociation of excitons. However, close to $T = T_0$, a stepwise rise in the NBE emission intensity is observed simultaneously with the quenching of the BL band (Fig. 7). The only plausible explanation for this rise in intensity is the thermal release of holes from the Zn$_{Ga}$ acceptor and their subsequent redistribution between all the other recombination channels. From the value of the step in the NBE emission (about an order of magnitude) we can quickly estimate[10] that the absolute IQE of the BL band is about 90%. A more accurate value can be obtained by fitting the temperature dependence of the NBE emission intensity with Eq. (17). The temperature dependence of I_{30}^{PL} in this equation is simulated with Eq. (14) in which two activation energies correspond to dissociation of free excitons at $T < T_0$ ($E_1 = 25$ meV) and unknown process involving apparent thermal quenching with $E_1 = 100$ meV at higher temperatures. The latter is clearly visible as a new slope of the NBE emission intensity decrease at $T >> T_0$. The best fit of the $I_3^{PL}(T)$ dependence (right scale) with Eq. (17) for the NBE band is shown in Fig. 7 with a green solid curve labeled as η_3. From this fit, we find $\eta_{10} = 0.95$ for the absolute IQE of the BL band in this sample. The parameter η_{10} for other samples was estimated using the same procedure, and the values are listed in column 5 of Table II. For sample 2015, the $I_3^{PL}(T)$ dependence increased by at most a factor of two from the $I_{30}^{PL}(T)$ dependence in the region of the quenching of the BL band, indicating that $\eta_{10} < 0.5$.

The estimate of η_{10} from the temperature dependence of the NBE band is more accurate than the one obtained from the $I_2^{PL}(T)$ dependence. The latter is less accurate because the quenching of the YL band with large activation energy starts at temperatures close to T_0, which may reduce the step by a value that is difficult to determine without

additional information about the YL band. For this reason, we assigned larger error bars for η_{10} determined from data for the YL band.

4. Enhancement of the NBE emission due to the saturation of the BL band at high excitation intensity

At low excitation intensity ($P_{exc} < 1\,\mathrm{W/cm^2}$), the IQE of the NBE emission is constant in samples with a high concentration of free electrons (Fig. 9); i.e., the NBE emission intensity increases linearly with the excitation intensity. This agrees with our theoretical prediction for the case when $n \approx n_0$ [see Eqs. (12) and (15)]. The IQE of the BL band is also constant at $P_{exc} < 1\,\mathrm{W/cm^2}$. At higher excitation densities, the BL band intensity starts saturating because of the limited number of the $\mathrm{Zn_{Ga}}$ acceptors. Remarkably, the IQE of the NBE emission increases, simultaneously with the decrease in the IQE of the BL band. The rise in the IQE of the NBE emission is expected to be followed by a constant IQE at higher excitation intensities; yet, they could not be achieved in our experiment. The $I_3^{PL}(P_{exc})$ dependence for the NBE band can be fit with Eq. (17) where the $\eta_1(P_0)$ is found from the fit of the dependence of the BL band intensity on excitation intensity with the method described in Sec. IV C. The fit with Eq. (17) allows us to find η_{10} (see Fig. 10). When η_{10} is close to unity, the accuracy of this method is high. The values of η_{10} found with this method are listed in the sixth column of Table II. This method has the advantage that I_{i0}^{PL} for the NBE emission is linearly proportional to G in the entire range of the excitation intensities, due to the high concentration of free electrons in degenerate n-type GaN samples. We were not able to obtain useful information with this method in application to sample 2015, because the concentration of free electrons was relatively low, and the $I_3^{PL}(P_{exc})$ dependence was slightly superlinear in the entire range of P_{exc} so that a small step in this dependence might remain unnoticed.

5. Error analysis

We have determined the absolute IQE of the BL band by using four independent methods. The results are summarized in Table II and Fig. 11. We can see that the IQE is higher in group A (uncapped layers) and it increases with increasing concentration of Zn. The value of 96% is the highest absolute IQE of PL reported for GaN in the limit of low excitation intensities. Very close values of η_{10} obtained from different methods provide confidence in the validity of these results.

The error in η_{10} has been estimated in each of the four approaches for each sample. The weighted average and its error (column 7 in Table II) were calculated following recommendations given in Ref. 18. The error is not symmetrical about the mean value because the accuracy in all the methods improves when η_{10} approaches unity. As an example, the error analysis for the sample with the highest IQE of PL (sample 1140) is given below.

From the fit of the temperature dependence of I_1^{PL} with Eq. (7) with fixed parameters $\tau_1 = 1.48$ μs and $C_{pA1} = 7 \times 10^{-7}\,\mathrm{cm^3/s}$, we find two fitting parameters: $\eta_{10} = 0.992$ and $E_{A1} = 290$ meV. They determine the posi-
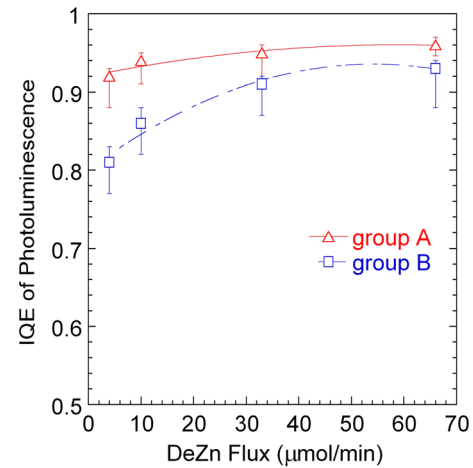

FIG. 11. Absolute IQE of the BL (η_{10}) in GaN:Si,Zn samples of groups A and B. $T = 200$ K and $P_{exc} = 0.0015\,\mathrm{W/cm^2}$. The lines are added to guide the eye.

tion and slope, respectively, of the high-temperature part of the dependence. Parameters C_{pA1} and τ_1 in Eq. (7) were estimated from independent experiments as $7 \times 10^{-7}\,\mathrm{cm^3/s}$, and 1.48 μs (see Secs. IIIC and VA1, and Table I). To find uncertainty in η_{10}, we varied E_{A1} from 240 to 340 meV, C_{pA1} - from 3×10^{-7} to $1.5 \times 10^{-6}\,\mathrm{cm^3/s}$, and τ_1 from 1.28 to 1.68 μs. By varying these three parameters in favorable and unfavorable directions to obtain a higher η_{10}, we have found $\eta_{10} = 0.999$ and $\eta_{10} = 0.89$, respectively, i.e., $\eta_{10} = 0.992^{+0.007}_{-0.10}$. In similar way, from analysis of the $I_2^{PL}(T)$, $I_3^{PL}(T)$, and $I_3^{PL}(P_0)$ dependencies, we have determined $\eta_{10} = 0.88^{+0.07}_{-0.20}$, $\eta_{10} = 0.88^{+0.05}_{-0.10}$, and $\eta_{10} = 0.97^{+0.01}_{-0.03}$, respectively, for sample 1140. Finally, the weighted average and propagated uncertainties are found[18] as $\eta_{10} = 0.96^{+0.01}_{-0.04}$ for this sample (Table II). Note that the size of the error bars decreases as the IQE approaches unity.

B. Determination of the concentration of defects and free electrons from photoluminescence

1. Determination of the electron concentration from photoluminescence

Concentration of free electrons can be determined from the following expression:[12,13]

$$n = (C_{n1}\tau_1)^{-1}. \quad (19)$$

Here, the PL lifetime τ_1 can be found from the time-resolved PL measurements. The electron-capture coefficient for the $\mathrm{Zn_{Ga}}$ acceptor, C_{n1}, is a characteristic of the acceptor, and therefore it should not be sample-dependent. Previously, by using Eq. (19), we have determined that $C_{n1} = 4 \times 10^{-13}\,\mathrm{cm^3/s}$ as the average value for the BL band in four undoped GaN samples grown by MOVPE.[9,12,13] The new experimental data presented in this work allow us to revise this value. By taking the electron concentration for the GaN:Si,Zn samples of group A from the Hall effect data and the lifetime of the BL band from the time-resolved PL data, we find that $C_{n1} = (1.5 \pm 0.2) \times 10^{-13}\,\mathrm{cm^3/s}$. This value is expected to be more accurate than the previously found value

of $C_{n1} = 4 \times 10^{-13}$ cm^3/s for the following reasons. The concentration of electrons in the top 0.2 μm-thick layer (where most of the PL originates) may be different from the concentration in the remaining part of the 2–5 μm-thick "bulk" GaN layer; or it may be shunted by a more conductive layer in nominally undoped GaN samples. However, in the GaN:Si,Zn samples studied in this work, the 0.2 μm-thick layer was isolated from the undoped GaN layer by an insulating AlGaN barrier. Moreover, the high concentration of electrons in the degenerate GaN:Si,Zn layers reduces the roles of the surface, interfaces, and contacts in the determination of the electron concentration by the Hall effect measurements. Furthermore, from the time-resolved PL data for degenerate GaN:Si,Zn samples at 200 K, the decay of the BL intensity, after a laser pulse, was close to an exponential dependence: closer than that in undoped GaN samples. This better justifies the use of Eq. (19) for degenerate material, because this expression is derived for the recombination of free electrons and bound holes, and may be invalid when the donor-acceptor pair recombination (characterized with a nonexponential decay of PL) is significant.

By using the new value of $C_{n1} = (1.5 \pm 0.2) \times 10^{-13}$ cm^3/s for the Zn$_{Ga}$ acceptor and the values of the BL lifetime at 200 K determined from the time-resolved PL measurements, we have estimated the concentration of free electrons in GaN:Si,Zn samples of groups A and B (Table I). In these samples, $n \approx 10^{19}$ cm^{-3}, and the variation in n, with increasing temperature from 200 to 300 K, is negligible.

The concentration of free electrons in Si-doped GaN (sample 2015) has been determined with this method as 4.5×10^{17} cm^{-3} at 200 K and extrapolated to be 6.5×10^{17} cm^{-3} at room temperature. This value is close to the value obtained from analysis of the temperature-dependent Hall effect data by using a two-layer model (3×10^{17} cm^{-3}).[8]

It may be informative to determine some other characteristics of the GaN:Si,Zn samples in the conditions of the steady-state PL. We can estimate the concentration of free holes from Eq. (4) with $Q_1 = 0$ for temperatures below 250 K. It is roughly 10^6 cm^{-3} for the lowest excitation density (10^{-5} W/cm^2) and $\sim 10^{13}$ cm^{-3} for the highest excitation density used in our experiments (100 W/cm^2). The lifetime of these holes in the valence band at temperatures below 250 K can be estimated from the following expression:

$$\tau_p = \frac{1}{\sum_{i=1}^{4} C_{pi}N_i} = \frac{\eta_{10}}{C_{p1}N_1}, \qquad (20)$$

which is on the order of 10^{-13} s. Such short lifetimes of free holes are due to their fast capture by the Zn$_{Ga}$ acceptors.

2. Determination of the concentrations of the Zn$_{Ga}$ and Si$_{Ga}$ centers from photoluminescence

We determined the concentration of the Zn$_{Ga}$ centers in GaN:Si,Zn and GaN:Si samples from the PL data by using two methods. In method 1, the value of N_1 was determined from the dependence of the BL band intensity on excitation intensity with the approach described in Sec. IV C. The IQE

of the BL band was plotted as a function of the excitation intensity P_0 (Fig. 10). The $\eta_1(P_0)$ dependence was fit with numerical integration of Eq. (18), in which $G(x) = \alpha P_0 e^{-\alpha x}$. With known parameters η_{10} and τ_1, the only fitting parameter is the concentration of the Zn$_{Ga}$ centers, N_1. The values found with this method are listed in column 6 of Table I and are shown in Fig. 12 for the samples of groups A and B.

In method 2, the value of N_1 is determined from the comparison of the IQE of the BL and NBE bands at 200 K. At low excitation intensity and at temperatures below the quenching of the BL band, $N_1^- = N_1$, $\eta_1 = \eta_{10}$, and $\eta_3 = \eta_{30}$. Then from Eqs. (8) and (12) we find

$$N_1 = \frac{\eta_{10}}{\eta_{30}} \frac{Bn}{C_{p1}}. \qquad (21)$$

The values of η_{10} were determined as the weighted average from the four methods described in Sec. V A (Table II). The values of η_{30} were estimated from the ratios of the integrated PL intensities for the NBE and BL bands multiplied by η_{10}, where both η_{10} and η_{30} were found at 200 K and at the low excitation intensity limit. The values of n were taken from the time-resolved PL data (Table I). Finally, we assumed that $B = 10^{-10}$ cm^3/s in GaN at 200 K. The value of B for band-to-band transitions in GaN is predicted to have the value between 2×10^{-11} and 4.5×10^{-10} cm^3/s for GaN at 300 K.[16,19–21] With decreasing temperature from 300 to 200 K, B is expected to increase by a factor of two.[16,19–21] Thus, the value of $B = 10^{-10}$ cm^3/s at 200 K is a reasonable value for our rough estimates.

Using the above-described methods, we estimated the concentrations of the Zn$_{Ga}$ centers in GaN:Si,Zn samples from groups A and B, and plotted them as a function of the Zn flow rate during growth (Fig. 12). Although we anticipate an error up to a factor of three for the *absolute* values of N_1 determined by each of the above methods, the *relative* values of the concentration of the Zn$_{Ga}$ centers in different samples have much better accuracy. We see that the
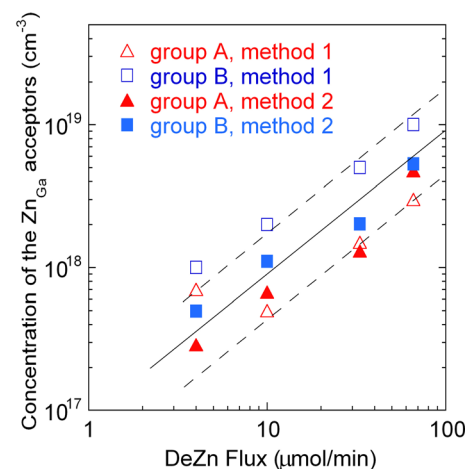

FIG. 12. Concentration of the Zn$_{Ga}$ acceptors in GaN:Si,Zn samples of series A and B calculated by two methods: from the $\eta_1(P_0)$ dependence (method 1) and from comparison of the IQE of the BL and NBE bands (method 2). $T = 200$ K, $C_{p1} = 7 \times 10^{-7}$ cm^3/s, $B = 10^{-10}$ cm^3/s, The values of n, η_{10}, η_{30}, and τ_1 are taken from Tables I and II. Solid and dashed lines show linear dependencies.

concentration of the Zn_{Ga} acceptors increases nearly linearly with DeZn flux and reaches the maximum value of $\sim 10^{19}$ cm^{-3} (Fig. 12).

Remarkably, the above-described methods allow us to estimate the concentration of the Zn_{Ga} centers when Zn is present in minute amounts, i.e., when its concentration cannot be determined by other methods. So, we obtained $N_1 = 3 \times 10^{15}$ cm^{-3} from method 1 for sample 2015, and an even smaller concentration of Zn is found in sample 1150 ($N_1 = 2 \times 10^{13}$ cm^{-3}) with method 2. Note that method 1 cannot be applied to sample 1150 because the BL band could not be reliably resolved at different excitation intensities needed to plot the $I_1^{PL}(P_0)$ dependence. On the other hand, method 2 appears to be accurate only for samples with a high concentration of free electrons, when $n \approx n_0$. For these samples, band-to-band recombination may dominate over the exciton recombination, at least at 200–300 K, and the surface effects (responsible for the near-surface depletion region) are negligible due to a very small depletion region width.

To find the concentration of the Si_{Ga} centers, we need to add N_1 to n: $N_{Si} = N_1 + n$. For all the samples of groups A and B, the concentration of the Si_{Ga} centers is about 10^{19} cm^{-3}, which is the same as in the sample grown in similar conditions but without Zn doping (sample 1150). Such a high concentration of shallow donors agrees with the large width of the NBE emission band at 200 K [compare the shape of the NBE band for samples 2015 and 1150 in Fig. 5 and also for GaN:Si,Zn samples of group A in Fig. 3(a)]. Note that the total concentrations of Si and Zn impurities in the GaN:Si,Zn layer may be higher than the concentrations of the Si_{Ga} and Zn_{Ga} centers, respectively, because not all impurities occupy substitution positions.

C. Other defects in GaN:Si,Zn

We assume that the YL band in the GaN samples heavily doped with Si is associated with the Si-related defects, and not with C or the $V_{Ga}O_N$ complex, where V_{Ga} is the Ga vacancy.[9] This assumption is based on the observation of different activation energies for thermal quenching of the YL band in undoped GaN samples[12] and Si-doped GaN samples. We propose that this defect is the $V_{Ga}Si_{Ga}$ complex. Although it is predicted that the $V_{Ga}Si_{Ga}$ complex is not as stable as the $V_{Ga}O_N$ complex in GaN,[22] the very high concentration of the Si_{Ga} donors may lead to significant concentrations of this defect. The situation appears to be very similar to the 1.2 eV band in GaAs which is attributed to the $V_{Ga}D$ complexes with D being the shallow donors substituting for the Ga site (Si_{Ga}, Ge_{Ga}, and Sn_{GA}) or As site (Te_{As}, S_{As}, Se_{As}).[23,24] Similar to the $V_{Ga}D$ complexes in GaAs, it is expected that the electronic structure of the Ga vacancy in GaN dominates the electronic structure of the $V_{Ga}D$ complexes involving a shallow donor.[22]

The very high IQE of PL observed in this work does not contradict the relatively high density of threading dislocations, on the order of 10^9 cm^{-2}, expected for GaN layers grown on sapphire by MOVPE. While the dislocations are commonly considered as the main source of nonradiative

recombination in GaN, the Zn acceptors with concentration above 10^{18} cm^{-3} and hole-capture cross-section of $\sim 10^{-13}$ cm^2 (Ref. 9), can successfully compete with the nonradiative channel for the capture of minority carriers (holes), provided that the doping does not create point nonradiative defects in large numbers.

VI. SUMMARY

We have fabricated high quality MOVPE GaN layers co-doped with silicon and zinc and have used several approaches to determine the absolute IQE of PL. Namely, (i) the characteristic temperature T_0 at which the thermal quenching of the BL band begins; (ii) the value of the increase in intensity of the YL and NBE bands caused by the quenching of the BL band; and (iii) the value of the rise of the relative IQE for the exciton band caused by a decrease of the BL band efficiency at high excitation intensities. With these independent approaches, we have estimated the absolute IQE of the BL band as $\eta_{10} = 0.81 - 0.96$ in several GaN:Si,Zn samples at $T < 250$ K and low excitation intensity. The methods used here are very accurate when the IQE approaches unity since the size of the effect (e.g., an increase of the PL intensity for all of the PL bands caused by a quenching of a PL band with a high IQE) is very large compared to the errors in modeling the $I_{i0}^{PL}(T)$ or $I_{i0}^{PL}(P_0)$ dependencies. We have also determined the concentration of free electrons and estimated the concentrations of the Zn_{Ga} and Si_{Ga} centers in these samples from the PL measurements.

ACKNOWLEDGMENTS

[1]M. A. Reshchikov, *Internal Quantum Efficiency of Photoluminescence in Wide-Bandgap Semiconductors, Chapter in Photoluminescence: Applications, Types and Efficacy*, edited by M. A. Case and B. C. Stout (Nova Science Publishers, Inc., New York, 2012), pp. 53–120, ISBN: 978-1-61942-426-5.

[2]H. Y. Ryu, K. H. Ha, J. H. Chae, K. S. Kim, J. S. Son, O. H. Nam, Y. J. Park, and J. I. Shim, Appl. Phys. Lett. **89**, 171106 (2006).

[3]Q. Dai, M. F. Schubert, M. H. Kim, J. K. Kim, E. F. Schubert, D. D. Koleske, M. H. Crawford, S. R. Lee, A. J. Fischer, G. Thaler, and M. A. Banas, Appl. Phys. Lett. **94**, 111109 (2009).

[4]X. Ni, J. Lee, M. Wu, X. Li, R. Shimada, Ü. Özgür, A. A. Baski, H. Morkoç, T. Paskova, G. Mulholland, and K. R. Evans, Appl. Phys. Lett. **95**, 101106 (2009).

[5]H. Yoshida, M. Kuwabara, Y. Yamashita, K. Uchiyama, and H. Kan, Appl. Phys. Lett. **96**, 211122 (2010).

[6]M. A. Reshchikov, A. G. Willyard, A. Behrends, A. Bakin, and A. Waag, Appl. Phys. Lett. **99**, 171107 (2011).

[7]D. C. Look and R. J. Molnar, Appl. Phys. Lett. **70**, 3377 (1997).

[8]J. D. McNamara, M. Foussekis, H. Liu, H. Morkoç, M. A. Reshchikov, and A. A. Baski, "Temperature Dependent Behavior of the SPV for n-type GaN," Proc. SPIE **8262**, 826213 (2012).

[9]M. A. Reshchikov and H. Morkoç, J. Appl. Phys. **97**, 061301 (2005).

[10]M. A. Reshchikov, A. Kvasov, T. McMullen, M. F. Bishop, A. Usikov, V. Soukhoveev, and V. A. Dmitriev, Phys. Rev. B **84**, 075212 (2011).

[11]M. A. Reshchikov, H. Morkoç, R. J. Molnar, D. Tsvetkov, and V. Dmitriev, Mater. Res. Soc. Symp. Proc. **743**, L11.1 (2003).

[12]M. A. Reshchikov and R. Y. Korotkov, Phys. Rev. B **64**, 115205 (2001).

[13]R. Y. Korotkov, M. A. Reshchikov, and B. W. Wessels, Physica B **325**, 1–7 (2003).

[14]W. Shockley and J. W. T. Read, Phys. Rev. **87**, 835 (1952).

[15]V. N. Abakumov, V. I. Perel, and I. N. Yassievich, *Nonradiative Recombinations in Semiconductors* (Elsevier, Amsterdam, 1991).

[16]A. Dmitriev and A. Oruzheinikov, J. Appl. Phys. **86**, 3241 (1999).

[17]M. A. Reshchikov, Appl. Phys. Lett. **88**, 202104 (2006).

[18]J. R. Taylor, *An Introduction to Error Analysis*, second ed. (University Science Books, Sausalito, CA, 1997).

[19]T. Malinauskas, K. Jaračiūnas, R. Aleksiejunas, D. Gogova, B. Monemar, B. Beamont, and P. Gibart, Phys. Status Solidi B **243**, 1426 (2006).

[20]J. S. Im, A. Moritz, F. Steuber, V. Härle, F. Scholz, and A. Hangleiter, Appl. Phys. Lett. **70**, 631 (1997).

[21]O. Brandt, H.-J. Wünsche, H. Yang, R. Klann, J. R. Müllhäuser, and K. H. Ploog, J. Cryst. Growth **189–190**, 790 (1998).

[22]J. Neugebauer and C. G. Van de Walle, Appl. Phys. Lett. **69**, 503 (1996).

[23]E. W. Williams, Phys. Rev. **168**, 922 (1968).

[24]N. S. Averkiev, A. A. Gutkin, E. B. Osipov, M. A. Reshchikov, and V. R. Sosnovskii, Defect Diffus. Forum **103–105**, 31 (1993).